

Massive Connectivity with Massive MIMO—Part II: Achievable Rate Characterization

Liang Liu, *Member, IEEE* and Wei Yu, *Fellow, IEEE*

Abstract—This two-part paper aims to quantify the cost of device activity detection in an uplink massive connectivity scenario with a large number of devices but device activities are sporadic. Part I of this paper shows that in an asymptotic massive multiple-input multiple-output (MIMO) regime, device activity detection can always be made perfect. Part II of this paper subsequently shows that despite the perfect device activity detection, there is nevertheless significant cost due to device detection in terms of overall achievable rate, because of the fact that non-orthogonal pilot sequences have to be used in order to accommodate the large number of potential devices, resulting in significantly larger channel estimation error as compared to conventional massive MIMO systems with orthogonal pilots. Specifically, this paper characterizes each active user’s achievable rate using random matrix theory under either maximal-ratio combining (MRC) or minimum mean-squared error (MMSE) receive beamforming at the base-station (BS), assuming the statistics of their estimated channels as derived in Part I. The characterization of user rate also allows the optimization of pilot sequences length. Moreover, in contrast to the conventional massive MIMO system, the MMSE beamforming is shown to achieve much higher rate than the MRC beamforming for the massive connectivity scenario under consideration. Finally, this paper illustrates the necessity of user scheduling for rate maximization when the number of active users is larger than the number of antennas at the BS.

Index Terms—Beamforming, massive connectivity, massive multiple-input multiple-output (MIMO), random matrix theory, large-system analysis, Internet-of-Things (IoT), machine-type communications (MTC).

I. INTRODUCTION

A. Motivation

Motivated by the emerging Internet-of-Things (IoT) and machine-type communications (MTC) applications, this two-part paper studies the uplink communication in a massive multiple-input multiple-output (MIMO) single-cell system, in which a base-station (BS) is equipped with a large number of antennas to serve a massive number of devices

Manuscript received June 17, 2017, revised November 9, 2017 and January 30, 2018, accepted March 8, 2018. The materials in this paper have been presented in part at the IEEE International Symposium on Information Theory (ISIT), Aachen, Germany, July 2017 [1]. The associate editor coordinating the review of this paper and approving it for publication was Dr. Mathini Sellathurai. This work is supported by Natural Sciences and Engineering Research Council (NSERC) of Canada via a discovery grant, a Steacie Memorial Fellowship and the Canada Research Chairs program.

The authors are with The Edward S. Rogers Sr. Department of Electrical and Computer Engineering, University of Toronto, Toronto, Ontario, Canada, M5S3G4, (e-mails:lianguot.liu@utoronto.ca; weiyu@comm.utoronto.ca).

with sporadic traffic. Specifically, the BS is equipped with M antennas, serving N potential devices, out of which K are active at any given time. A two-phase multiple-access scheme is adopted in which within each coherence time of length T , the active users send their pilot sequences during the first $L < T$ symbols for device activity detection and channel estimation in the first phase, while send their data messages during the remaining $T - L$ symbols in the second phase.

A key challenge of the above system is that due to the limited coherence time, only non-orthogonal pilot sequences can be assigned to the users, as typically $N \gg L$. The main objective of Part I of this paper [2] is to quantify the performance of device activity detection and channel estimation when *randomly generated non-orthogonal pilot sequences* are assigned for each device. Part II of this paper examines its impact on the overall achievable data rate for this massive connectivity system with massive MIMO.

Part I of this paper [2] shows that the user activity detection and channel estimation problem in the first phase can be cast as a compressed sensing problem that takes advantage of the sparsity in device activity, for which the approximate message passing (AMP) algorithm [3]–[6] can be used to solve the above problem. Specifically, Part I of this paper designs a minimum mean-squared error (MMSE) denoiser in a vector form of the AMP algorithm for user activity detection and channel estimation based on the statistics of the channel, and shows that in certain asymptotic regime where K, N, L all go to infinity, the probabilities of missed detection and false alarm as well as the statistical distributions of the active users’ estimated channels can be characterized analytically. Interestingly, it is shown that the MMSE-based AMP algorithm is capable of driving the user detection error probability down to zero as the number of BS antennas M goes to infinity. Thus, massive MIMO is naturally suited for massive connectivity.

Part II of the paper leverages the above perfect user activity detection result as well as the statistical distributions of the estimated channels to characterize in closed-form the overall achievable rates under the aforementioned two-phase transmission protocol with either the maximal-ratio combining (MRC) or the MMSE beamforming at the BS, again in the massive MIMO regime as M goes to infinity. Our main conclusion is that despite perfect detection, there is nevertheless significant cost on user achievable rate due to massive device detection because the use of non-orthogonal

pilot sequences results in larger channel estimation errors.

B. Prior Work

Massive MIMO systems [7], where each BS is equipped with a large number (sometimes in the order of 100's) of antennas, have emerged as a key technology for achieving dramatic spectral efficiency gains in future wireless systems. In a single-cell system where the number of antennas at the BS is much larger than that of the users, the channels of different users become asymptotically orthogonal under the so-called "favorable" propagation conditions [7]. As a result, simple matched filter (MF) processing, such as maximal-ratio transmission (MRT) in the downlink and MRC in the uplink, is already asymptotically optimal for maximizing the user rate, assuming perfect channel state information (CSI) [7]. Moreover, it is shown in [8] that each single-antenna user in a massive MIMO system can scale down its transmit power proportional to the number of antennas at the BS to get the same rate performance as a corresponding single-input single-output (SISO) system, assuming perfect CSI.

Despite its promises, massive MIMO system is also faced with many practical challenges, chief among which is channel estimation [9]. Channel training for the uplink MIMO system should typically be done with orthogonal pilot sequences within each cell; further the optimal training length in time should be the same as the number of transmit antennas in uncorrelated Rayleigh fading channels [10]. With this channel training strategy, the user rates achieved by the MRC beamforming and MMSE beamforming at the BS are characterized in [8], [11] utilizing the random matrix theory, where it is shown that even with imperfect CSI, the throughput achieved by the MRC beamforming is very close to that of MMSE beamforming in the uplink massive MIMO system. We remark that channel training is even more challenging in the downlink massive MIMO system, especially when the system operates in the frequency-division duplex (FDD) mode where channel reciprocity does not hold between uplink and downlink. Many sophisticated schemes have been proposed for this long-standing problem in the downlink FDD massive MIMO system [9], [12]. Finally, we mention that in a multi-cell system, the non-orthogonality of the pilot sequences in nearby cells causes pilot contamination, which then becomes the dominant impairment in the asymptotic massive MIMO regime [7].

In contrast to the conventional massive MIMO literature, this paper points out that channel training can be a limiting factor even in the single-cell uplink scenario, when massive number of devices are involved. This is because when the total number of devices is much larger than the number of BS antennas, it is impossible to assign orthogonal pilot sequences to each device. Part I of this paper [2] deals with device activity detection. In this Part II of the paper, we aim to quantify the cost of non-orthogonal pilots for channel estimation and subsequently the overall achievable rate. One of the consequences of our result is that MMSE beamforming is necessary for maximizing the user rate,

because of the fact that the inter-user interference cannot be effectively canceled by a simple MRC operation when the number of active users is comparable to the number of antennas at the BS.

C. Main Contributions

This two-part paper provides an analytical performance characterization of the two-phase transmission protocol in a single-cell massive connectivity scenario with massive MIMO, in which the active users send their non-orthogonal pilot sequences to the BS simultaneously for user activity detection and channel estimation in the first phase, then transmit data to the BS for information decoding in the second phase, within the same coherence time. The main contributions of Part II of this paper are as follows.

Based on the user activity detection and channel estimation statistics results of Part I of this paper and also based on techniques from random matrix theory, we characterize the user achievable rate for both the cases of MRC and MMSE beamforming at the BS, in an asymptotic limit where the number of antennas at the BS and the number of users both go to infinity, while keeping their ratio fixed. By comparing to the case with prior information of user activity at the BS, it is shown that despite the guaranteed success in activity detection, the non-orthogonality of pilot sequences can nevertheless lead to significantly larger channel estimation error as compared to the conventional massive MIMO system, thus limiting the overall achievable transmission rate. We quantify this cost and illustrate that the optimal pilot sequence length in a massive connectivity system should be longer than that in conventional massive MIMO system for maximizing the overall transmission rate.

This paper shows that the massive connectivity system also possesses other fundamental differences as compared to the conventional massive MIMO system with a small number of users. First, the user rate is finite due to inter-user interference, even in a single-cell massive MIMO system with infinite number of antennas and without pilot contamination from other cells. Second, the user rate achieved by the MMSE beamforming at the BS is significantly higher than that achieved by the MRC beamforming. At last, we show that in an overloaded system where the number of active users is much larger than that of the antennas at the BS, user scheduling can significantly improve the overall transmission rate if the MMSE beamforming is applied at the BS.

D. Organization

The rest of Part II of this paper is organized as follows. Section II describes the system model for massive connectivity and introduces the two-phase transmission protocol for user detection, channel estimation, and data transmission. Section III reviews the vector AMP algorithm and its performance in terms of user activity detection and channel estimation derived in Part I of this paper; Section

IV analyzes user achievable rate with the MRC and MMSE beamforming at the BS with or without user scheduling; Section V investigates the cost of user activity detection on user rate; Sections VI and VII optimize the pilot sequence length and number of scheduled intervals to maximize the user sum rate, respectively; Section VIII provides the numerical simulation results pertaining to user achievable rate. Finally, Section IX concludes the paper and points out several future directions.

E. Notation

Scalars are denoted by lower-case letters, vectors by bold-face lower-case letters, and matrices by bold-face upper-case letters. The identity matrix and the all-zero matrix of appropriate dimensions are denoted as \mathbf{I} and $\mathbf{0}$, respectively. For a matrix \mathbf{M} of arbitrary size, \mathbf{M}^H and \mathbf{M}^T denote its conjugate transpose and transpose, respectively. The expectation operator is denoted as $\mathbb{E}[\cdot]$. The distribution of a circularly symmetric complex Gaussian (CSCG) random vector with mean \mathbf{x} and covariance matrix Σ is denoted by $\mathcal{CN}(\mathbf{x}, \Sigma)$; the space of complex matrices of size $m \times n$ is denoted as $\mathbb{C}^{m \times n}$.

II. SYSTEM MODEL

The overall system model is as introduced in Part I of this two-part paper [2]. The channel input-output relationship for the uplink communication in a single cell consisting of N single-antenna users and one BS with M antennas is given as:

$$\mathbf{y} = \sum_n \mathbf{h}_n \alpha_n x_n + \mathbf{z} = \sum_{k \in \mathcal{K}} \mathbf{h}_k x_k + \mathbf{z}, \quad (1)$$

where $x_n \in \mathbb{C}$ with a power $\mathbb{E}|x_n|^2 = \rho$ is the transmit signal of user n , $\mathbf{h}_n \in \mathbb{C}^{M \times 1} \sim \mathcal{CN}(\mathbf{0}, \beta_n \mathbf{I})$ denotes the complex uplink channel vector from user n to the BS with a path-loss exponent β_n known by the BS, $\mathbf{z} \in \mathbb{C}^{M \times 1} \sim \mathcal{CN}(\mathbf{0}, \sigma^2 \mathbf{I})$ is the additive white Gaussian noise (AWGN) vector at the BS, and $\mathbf{y} \in \mathbb{C}^{M \times 1}$ is the received signal. Here in (1), α_n 's are the user activity indicators used to model the sporadic traffic pattern of massive connectivity, i.e., $\alpha_n = 1$ if user n is active at one coherence time, and $\alpha_n = 0$ otherwise, $n = 1, \dots, N$. At last, \mathcal{K} is the set of active users within a coherence block, i.e., $\mathcal{K} = \{n : \alpha_n = 1, n = 1, \dots, N\}$, with a cardinality $K = |\mathcal{K}|$.

Within each coherence time with T symbols, we adopt the following two-phase multiple access scheme: in the first phase of length L symbols, the BS conducts user activity detection and channel estimation based on the pilot sequences from the active users; in the second phase, the BS decodes user messages based on the estimated channels in the previous phase. The transmitted signals of the active users are assumed to be synchronized in both phases. The key point here is that in a massive connectivity system with $N > L$, it is impossible to assign orthogonal pilots to all the potential users. In this paper, we assume a non-orthogonal pilot sequence assignment strategy in which each

user n is allocated to a pilot $\mathbf{a}_n \in \mathbb{C}^{L \times 1}$ whose entries are generated from independently and identically distributed (i.i.d.) complex Gaussian distribution with zero mean and variance $1/L$.

III. USER ACTIVITY DETECTION AND CHANNEL ESTIMATION IN MASSIVE MIMO REGIME

The AMP algorithm is effective for device activity detection and channel estimation for the massive connectivity scenario. This section first summarizes the main analysis in [2], then further derives an analytic expression for channel estimation error for system parameter regime of most interest, which is useful for subsequent characterization of the cost of non-orthogonal pilot sequences on user rate and for optimization of the pilot sequence length for rate maximization.

A. AMP for Activity Detection and Channel Estimation

Consider the first phase of massive device transmission in which each user sends its pilot sequence synchronously through the channel. Define ρ^{pilot} as the identical transmit power of the active users in the first transmission phase. The transmit signal of user n can be expressed as $\alpha_n \sqrt{\xi} \mathbf{a}_n$, where $\xi = L \rho^{\text{pilot}}$ denotes the total transmit energy of each active user in the first phase. The received signal at the BS is then

$$\mathbf{Y} = \sqrt{\xi} \mathbf{A} \mathbf{X} + \mathbf{Z}, \quad (2)$$

where $\mathbf{Y} \in \mathbb{C}^{L \times M}$ is the matrix of received signals across M antennas over L symbols, $\mathbf{A} = [\mathbf{a}_1, \dots, \mathbf{a}_N]$ is the collection of user pilot sequences, $\mathbf{X} = [\mathbf{x}_1, \dots, \mathbf{x}_N]^T$ is the collection of user equivalent channels $\mathbf{x}_n = \alpha_n \mathbf{h}_n$'s, and $\mathbf{Z} = [\mathbf{z}_1, \dots, \mathbf{z}_M]$ with $\mathbf{z}_m \sim \mathcal{CN}(\mathbf{0}, \sigma^2 \mathbf{I})$, $\forall m$, is the independent AWGN at the BS. As \mathbf{X} is row sparse, Part I of this paper proposes to use the MMSE-based vector AMP algorithm to recover \mathbf{X} based on the noisy observation \mathbf{Y} . More details on the implementation of the vector AMP algorithm can be found in [2].

The main result of [2] is an analytical characterization of the user activity detection and channel estimation performance using the vector AMP algorithm in the asymptotic regime where $L, K, N \rightarrow \infty$, while their ratios converge to some fixed positive values $N/L \rightarrow \omega$ and $K/N \rightarrow \epsilon$ with $\omega, \epsilon \in (0, \infty)$, while keeping the total transmit power fixed at ξ . Specifically, for user activity detection, we show that in the above asymptotic regime, the probabilities of missed detection (a user is active but is declared as inactive) and false alarm (a user is inactive but is declared as active) by the MMSE-based AMP algorithm both converge to zero exponentially as the number of antennas at the BS, i.e., M , goes to infinity.

Moreover, for channel estimation, after the convergence of the vector AMP algorithm, the covariance matrices of the estimated channel of an active user $k \in \mathcal{K}$, denoted by $\hat{\mathbf{h}}_k$,

and the corresponding channel estimation error, denoted by $\Delta \mathbf{h}_k = \mathbf{h}_k - \hat{\mathbf{h}}_k$, are given, respectively, by

$$\text{Cov}(\hat{\mathbf{h}}_k, \hat{\mathbf{h}}_k) = v_k(M) \mathbf{I}, \quad (3)$$

$$\text{Cov}(\Delta \mathbf{h}_k, \Delta \mathbf{h}_k) = \Delta v_k(M) \mathbf{I}, \quad (4)$$

where $v_k(M)$ and $\Delta v_k(M)$ respectively converge to as the number of antennas at the BS goes to infinity:

$$\lim_{M \rightarrow \infty} v_k(M) = \frac{\beta_k^2}{\beta_k + \tau_\infty^2}, \quad (5)$$

$$\lim_{M \rightarrow \infty} \Delta v_k(M) = \frac{\beta_k \tau_\infty^2}{\beta_k + \tau_\infty^2}. \quad (6)$$

In (5) and (6), τ_∞^2 is the fixed-point solution to the following simplified state evolution of the AMP algorithm as $M \rightarrow \infty$:

$$\tau_0^2 = \frac{\sigma^2}{\xi} + \omega \epsilon \mathbb{E}_\beta[\beta], \quad (7)$$

$$\tau_{t+1}^2 = \frac{\sigma^2}{\xi} + \omega \epsilon \mathbb{E}_\beta \left[\frac{\beta \tau_t^2}{\beta + \tau_t^2} \right], \quad t \geq 0. \quad (8)$$

We emphasize that although the above results are obtained in the asymptotic regimes where N, K, L go to infinity, they can be used to predict the performance of practical systems with finite but large N, K, L, M accurately. In particular, for a practical system with parameters $\rho^{\text{pilot}}, L, K, N$ and pathloss β_k for each user k , we simply set

$$\xi = L \rho^{\text{pilot}}, \quad \epsilon = \frac{K}{N}, \quad \omega = \frac{N}{L}, \quad (9)$$

in order to run the simplified state evolution (7)-(8) to obtain τ_∞^2 and subsequently v_k and Δv_k for each user k . Although the above asymptotic results are obtained in the limit of large M , they already corroborate well with the simulation results as shown in Part I of this paper [2] for practical values of $M = 16$ and $M = 64$. In this Part II of the paper, we assume the above characterization of the channel estimation error in order to analytically characterize the overall achievable rate.

B. High SNR Characterization of Channel Estimation

A key step in obtaining the statistics of the channel estimation error according to (3)–(6) is in identifying the fixed point τ_∞^2 of the state evolution (8). In general, the fixed point is a complicated function of the system parameter. But in certain regime of practical interest, simple analytic characterization of the fixed point can be obtained.

Observe that in practice, the vector AMP algorithm for device activity detection and channel estimation should work in the regime of $\omega \epsilon < 1$, i.e., $L > K$, in order to control the channel estimation error. Thus, the behavior of τ_∞^2 when $L > K$ is of most interest. Further, the iterative state evolution simplifies considerably in the high signal-to-noise ratio (SNR) limit. The first technical result of this paper is a high SNR characterization of the fixed point.

Theorem 1: Suppose that $\omega \epsilon < 1$, i.e., $L > K$. Then, there is a unique fixed-point solution τ_∞^2 to (8), which satisfies

$$\frac{\sigma^2}{\xi} \leq \tau_\infty^2 \leq \frac{\sigma^2}{\xi(1 - \omega \epsilon)}. \quad (10)$$

Moreover, suppose that the channel path-loss variable β is bounded below, i.e., $\beta \geq \beta_{\min}$, for some positive β_{\min} . Then, in the SNR regime where $\frac{\xi \beta_{\min}}{\sigma^2} \rightarrow \infty$, the unique fixed-point solution to (8) is given by

$$\tau_\infty^2 \rightarrow \frac{\sigma^2}{\xi(1 - \omega \epsilon)}. \quad (11)$$

Proof: Please refer to Appendix A. \blacksquare

Note that in a single-cell system without inter-cell interference, the SNR of the even cell-edge user is typically high within reasonable range. As a result, the approximation of τ_∞^2 given in (11) is expected to be accurate in the single-cell system, as verified later in this paper by simulations. Moreover, (10) shows that the upper bound of τ_∞^2 is $\sigma^2/\xi(1 - \omega \epsilon)$. Therefore, the asymptotic high-SNR limit obtained in (11) is also the worst-case noise power, and all the results based on this approximation can be viewed as performance lower bound for any value of SNR.

The main consequence of Theorem 1 is that under practical system parameters $K, L, N, \rho^{\text{pilot}}$, and for reasonably large M (such as $M = 16$ or 64), the covariance matrices of the estimated channel and the channel estimation error for user k , resulting from the use of AMP for joint device detection and channel estimation, are in the form of (3) and (4), in which v_k and Δv_k can be approximated respectively as:

$$v_k = \frac{\beta_k^2}{\beta_k + \frac{\sigma^2}{\rho^{\text{pilot}}(L-K)}}, \quad (12)$$

and

$$\Delta v_k = \frac{\beta_k \frac{\sigma^2}{\rho^{\text{pilot}}(L-K)}}{\beta_k + \frac{\sigma^2}{\rho^{\text{pilot}}(L-K)}}, \quad (13)$$

where we have used (9). Curiously, the above expressions are independent of N . This is because device activity detection is already perfect in the massive MIMO regime; the channel estimation error is mainly due to the non-orthogonality of the pilot sequences of the K active users.

IV. ACHIEVABLE RATE FOR MASSIVE CONNECTIVITY

We are now ready to use the channel estimation error characterization in the previous section to evaluate the achievable data transmission rate in the second phase while accounting for the channel estimation error, in the massive MIMO regime. As user activity detection is perfect in the massive MIMO regime in the first phase, we focus on an equivalent wireless system in the second phase consisting of only K active users that simultaneously transmit their data to the BS in the uplink. Moreover, for these users, we utilize the covariance matrices of the estimated channels and channel estimation errors as given in (3)-(6), or as in the high SNR regime, (12)-(13).

In this paper, we choose to study the user achievable rate in certain asymptotic regime, where not only M goes to infinity, but also K goes to infinity, while their ratio is kept fixed, i.e., $K/M \rightarrow \mu$ with $\mu \in (0, \infty)$. Note that this is

a different asymptotic regime as in the analysis of the first phase, but we justify by pointing out that both analyses are ultimately intended for performance projection of system with finite parameters. Had we followed the asymptotic regime of the analysis of the first phase, where K goes to infinity first for each finite M , then let M go to infinity, we would have obtained zero user rate, which is not of practical interest. Our present approach of letting both K and M go to infinity in the analysis of the second phase, while simply assuming the channel estimation characterization of the first phase, is validated by simulation later in the paper. It also leads to valuable system insight by allowing performance comparison to the case with prior user activity information at the BS, i.e., the case with orthogonal pilot sequences assignment as widely assumed in the current massive MIMO literature.

A. Achievable Rates with MRC and MMSE Receivers

The equivalent baseband signal received at the BS for the second phase is expressed as

$$\mathbf{y} = \sum_{n \in \mathcal{K}} \mathbf{h}_n \sqrt{\rho^{\text{data}}} s_n + \mathbf{z}, \quad (14)$$

where $s_n \sim \mathcal{CN}(0, 1)$ denotes the transmit symbol of user $n \in \mathcal{K}$, which is modeled as a CSCG random variable with zero-mean and unit-variance, ρ^{data} denotes the identical transmit power of the active users in the second transmission phase, and $\mathbf{z} \sim \mathcal{CN}(\mathbf{0}, \sigma^2 \mathbf{I})$ denotes the AWGN at the BS.

The BS employs linear beamforming on the received signal \mathbf{y} for decoding user messages:

$$\begin{aligned} \hat{s}_k &= \mathbf{w}_k^H \left(\sum_{n \in \mathcal{K}} \mathbf{h}_n \sqrt{\rho^{\text{data}}} s_n + \mathbf{z} \right) \\ &= \mathbf{w}_k^H \hat{\mathbf{h}}_k \sqrt{\rho^{\text{data}}} s_k + \mathbf{w}_k^H \sum_{n \in \mathcal{K}, n \neq k} \hat{\mathbf{h}}_n \sqrt{\rho^{\text{data}}} s_n \\ &\quad + \mathbf{w}_k^H \sum_{n \in \mathcal{K}} \Delta \mathbf{h}_n \sqrt{\rho^{\text{data}}} s_n + \mathbf{w}_k^H \mathbf{z}, \quad \forall k \in \mathcal{K}, \end{aligned} \quad (15)$$

where $\mathbf{w}_k \in \mathbb{C}^{M \times 1}$ denotes the beamforming vector for the active user $k \in \mathcal{K}$. In the above signal model, the BS views the estimated channels as the true channels, and treats the term due to the channel estimation error, i.e., $\mathbf{w}_k^H \sum_{n \in \mathcal{K}} \Delta \mathbf{h}_n \sqrt{\rho^{\text{data}}} s_n$, as additional noise.

Assume that the estimated channel and channel estimation error for each active user k are Gaussian distributed with the covariance matrices given in (3)-(6), i.e., $\hat{\mathbf{h}}_k \sim \mathcal{CN}(\mathbf{0}, \frac{\beta_k^2}{\beta_k + \tau_\infty^2} \mathbf{I})$ and $\Delta \mathbf{h}_k \sim \mathcal{CN}(\mathbf{0}, \frac{\beta_k \tau_\infty^2}{\beta_k + \tau_\infty^2} \mathbf{I})$. This can be justified by the fact that in the asymptotic massive MIMO regime, user activity detection is perfect and the MMSE denoiser as given in Theorem 1 of Part I asymptotically

becomes a linear MMSE channel estimator for the active users. As a result, the estimated channels from the AMP algorithm can be assumed to be close to Gaussian in the massive MIMO limit. Following the standard bounding technique based on the worst case uncorrelated noise [10], the uplink achievable rate of active user k can be written down as

$$R_k = \frac{T-L}{T} \log_2(1 + \gamma_k), \quad \forall k, \quad (16)$$

where the signal-to-interference-plus-noise ratio (SINR) of user k given the channel realization is shown in (17) on the bottom of the page.

This paper considers two different receive beamforming strategies, namely the MRC beamforming and MMSE beamforming, which are respectively defined as

$$\mathbf{w}_k^{\text{MRC}} = \hat{\mathbf{h}}_k, \quad (18)$$

$$\mathbf{w}_k^{\text{MMSE}} = \left(\sum_{n \in \mathcal{K}} \rho^{\text{data}} \hat{\mathbf{h}}_n \hat{\mathbf{h}}_n^H + \sum_{n \in \mathcal{K}} \frac{\rho^{\text{data}} \beta_n \tau_\infty^2}{\beta_n + \tau_\infty^2} \mathbf{I} + \sigma^2 \mathbf{I} \right)^{-1} \hat{\mathbf{h}}_k. \quad (19)$$

The following theorem characterizes the achievable rates of each user with the MRC beamforming and the MMSE beamforming, respectively, in our interested asymptotic regime.

Theorem 2: Consider an uplink massive MIMO system with M BS antennas serving K users. Assume that the estimated channel and channel estimation error for each active user k are Gaussian distributed with the covariance matrices given in (3)-(6), i.e., $\hat{\mathbf{h}}_k \sim \mathcal{CN}(\mathbf{0}, \frac{\beta_k^2}{\beta_k + \tau_\infty^2} \mathbf{I})$ and $\Delta \mathbf{h}_k \sim \mathcal{CN}(\mathbf{0}, \frac{\beta_k \tau_\infty^2}{\beta_k + \tau_\infty^2} \mathbf{I})$, $\forall k \in \mathcal{K}$. In the asymptotic regime where both K, M go infinity but with their ratio kept constant, i.e., $K/M \rightarrow \mu$ with $\mu \in (0, \infty)$, the achievable rate for each user, assuming MRC beamforming (18) at the BS, is given by (16), where

$$\gamma_k^{\text{MRC}} \rightarrow \frac{\beta_k^2}{\mu \mathbb{E}[\beta] (\beta_k + \tau_\infty^2)}, \quad \forall k. \quad (20)$$

The achievable rate for each active user, assuming MMSE beamforming (19) at the BS, is given by (16), where

$$\gamma_k^{\text{MMSE}} \rightarrow \frac{\beta_k^2}{\beta_k + \tau_\infty^2} \Gamma, \quad \forall k, \quad (21)$$

with Γ being the unique finite fixed-point solution of the following equation:

$$\Gamma = \frac{1}{\mu \mathbb{E} \left[\frac{\beta^2}{\beta + \tau_\infty^2 + \beta^2 \Gamma} \right] + \mu \mathbb{E} \left[\frac{\beta \tau_\infty^2}{\beta + \tau_\infty^2} \right]}. \quad (22)$$

$$\gamma_k = \frac{\rho^{\text{data}} |\mathbf{w}_k^H \hat{\mathbf{h}}_k|^2}{\rho^{\text{data}} \sum_{n \in \mathcal{K}, n \neq k} |\mathbf{w}_k^H \hat{\mathbf{h}}_n|^2 + \rho^{\text{data}} \|\mathbf{w}_k\|^2 \sum_{n \in \mathcal{K}} \frac{\beta_n \tau_\infty^2}{\beta_n + \tau_\infty^2} + \sigma^2 \|\mathbf{w}_k\|^2}. \quad (17)$$

Proof: Please refer to Appendix B. ■

We remark that given the perfect user detection and channel estimation characterization obtained in Part I of this paper [2], Theorem 2 can also be obtained based on the techniques used in [11]. Since we are considering a single-cell rather than multi-cell setting, we are able to provide a different and simpler proof in Appendix B. Note that this two-part paper studies a different system as compared to [11], since in [11] there are only K users who are assumed to be always active, while in our paper, K out of N users are active in each coherence interval, as result, the device activity detection step has impact on the channel estimation error, thus leading to more involved SINR expressions as compare to [11].

We also remark that if the channel estimation had been perfect, i.e., $\tau_\infty^2 = 0$ so that $\hat{\mathbf{h}}_k = \mathbf{h}_k, \forall k$, the above theorem reduces to known results in the literature. With the MRC receive beamforming at the BS, each user's SINR given in (20) in this case reduces to

$$\gamma_k^{\text{MRC}} \rightarrow \frac{\beta_k}{\mu \mathbb{E}[\beta]}. \quad (23)$$

This is the same result as in [13, Proposition 3.3].

Moreover, with the MMSE receive beamforming at the BS, Γ as given in (22) in the perfect channel estimation case reduces to the fixed-point solution to the following equation:

$$\Gamma = \frac{1}{\mu \mathbb{E} \left[\frac{\beta}{1 + \beta \Gamma} \right]}. \quad (24)$$

As a result, each user's SINR is the fixed-point solution to the following equation:

$$\gamma_k^{\text{MMSE}} = \beta_k \Gamma = \frac{\beta_k}{\mu \mathbb{E} \left[\frac{\beta}{1 + \beta \Gamma} \right]} = \frac{\beta_k}{\mu \mathbb{E} \left[\frac{\beta \beta_k}{\beta_k + \beta \gamma_k^{\text{MMSE}}} \right]}, \quad (25)$$

which is the same result as in [13, Theorem 3.1].

Observe that the user achievable rates under both the MRC and MMSE beamforming strategies as shown in Theorem 2 are finite, in contrast to the conventional single-cell (thus without pilot contamination) massive MIMO scenario with a small number of users, where the user achievable rates go to infinite in the massive MIMO limit [7], [8]. This is because in a massive connectivity scenario where the number of users is comparable with the number of antennas at the BS, the total inter-user interference power seen by each user is comparable to that of its desired signal, due to the fact that although each interference alone is very weak due to the channel asymptotic orthogonality, there are a large number of interference sources in the system, resulting in finite achievable rate.

It is also worth noting that the MRC beamforming is optimal in the conventional single-cell massive MIMO system in the asymptotic limit of large number of BS antennas but finite number of users, because the user channels become orthogonal with each other in the limit, thus the inter-user interference is asymptotically zero. But this is not the case for the massive connectivity scenario under consideration in

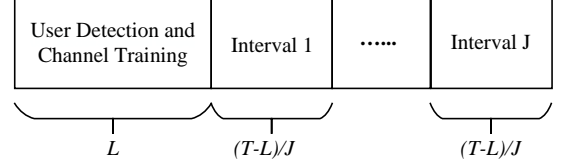


Fig. 1. User scheduling strategy in an overloaded system.

which the number of users also goes to infinity. Because of the large number of interference sources in the system, the inter-user interference remains significant with MRC beamforming. In contrast, the MMSE beamforming strategy can more effectively control the inter-user interference. As a result, there is a performance gap between the MRC and MMSE beamforming strategies in the massive connectivity scenario.

B. User Scheduling for Overloaded System

The above analysis assumes that in the second phase, all the K active users transmit simultaneously to the BS. It is worth noting that in an overloaded system where the number of active users is larger than the number of the antennas at the BS, i.e., $\mu = K/M > 1$, in general we should further divide the second phase into J intervals such that in each interval only K/J users are scheduled for information transmission in order to control the inter-user interference, as shown in Fig. 1. In the following, we formulate the user achievable rates with scheduling in an overloaded system. The optimization over J is treated later in Section VII. Note that we assume a finite J such that K/J goes to infinity thus Theorem 2 still applies to each scheduled interval.

First, consider the case with the MRC beamforming at the BS. Note that for each interval the ratio between the numbers of the scheduled users and the antennas at the BS is reduced to $K/(JM) = \mu/J$. Moreover, the transmission time¹ for each active user is reduced to $(T - L)/J$. As a result, the rate expression for each active user becomes

$$R_k^{\text{MRC,SC}} = \frac{T - L}{TJ} \log_2(1 + \gamma_k^{\text{MRC,SC}}), \quad \forall k, \quad (26)$$

where the SINR is

$$\gamma_k^{\text{MRC,SC}} \rightarrow \frac{J\beta_k^2}{\mu \mathbb{E}[\beta](\beta_k + \tau_\infty^2)}. \quad (27)$$

Moreover, with the MMSE beamforming at the BS, the achievable rate for each active user is given by

$$R_k^{\text{MMSE,SC}} = \frac{T - L}{TJ} \log_2(1 + \gamma_k^{\text{MMSE,SC}}), \quad \forall k, \quad (28)$$

where the SINR is

$$\gamma_k^{\text{MMSE,SC}} \rightarrow \frac{\beta_k^2}{\beta_k + \tau_\infty^2} \Gamma, \quad (29)$$

¹We ignore the overhead for informing each active user of the index of its scheduled interval since it is negligible compared to L .

with Γ the fixed-point solution to

$$\Gamma = \frac{J}{\mu\mathbb{E}\left[\frac{\beta^2}{\beta+\tau_\infty^2+\beta^2\Gamma}\right] + \mu\mathbb{E}\left[\frac{\beta\tau_\infty^2}{\beta+\tau_\infty^2}\right]}. \quad (30)$$

C. High SNR Approximation of User Rate

When the overall system operates in the regime $L > K$, and if we assume high SNR, we can use (11) to approximate τ_∞^2 in the above rate expressions. In this case, (11) can be further simplified as $\tau_\infty^2 = \frac{\sigma^2}{\rho^{\text{pilot}}(L-K)}$. Further, for practical systems with finite K and M , expressions such as $\mu\mathbb{E}[\beta]$ can be replaced by their empirical average, i.e., $\frac{1}{M} \sum_{k \in \mathcal{K}} \beta_k$.

With the above approximations, for the case without user scheduling, the user SINRs using the MRC and the MMSE receive beamforming as given in (20) and (21), respectively, reduce to

$$\gamma_k^{\text{MRC}} \approx \frac{\beta_k^2}{\frac{1}{M} \sum_{n \in \mathcal{K}} \beta_n (\beta_k + \frac{\sigma^2}{\rho^{\text{pilot}}(L-K)})}, \quad \forall k, \quad (31)$$

$$\gamma_k^{\text{MMSE}} \approx \frac{\beta_k^2}{\beta_k + \frac{\sigma^2}{\rho^{\text{pilot}}(L-K)}} \Gamma, \quad \forall k, \quad (32)$$

with Γ being the unique solution to the following equation:

$$\frac{1}{\Gamma} = \frac{1}{M} \sum_{n \in \mathcal{K}} \frac{\beta_n^2}{\beta_n + \frac{\sigma^2}{\rho^{\text{pilot}}(L-K)} + \beta_n^2 \Gamma} + \frac{1}{M} \sum_{n \in \mathcal{K}} \frac{\frac{\beta_n \sigma^2}{\rho^{\text{pilot}}(L-K)}}{\beta_n + \frac{\sigma^2}{\rho^{\text{pilot}}(L-K)}}. \quad (33)$$

For the case with user scheduling, we have:

$$\gamma_k^{\text{MRC,SC}} \approx \frac{J\beta_k^2}{\frac{1}{M} \sum_{n \in \mathcal{K}} \beta_n (\beta_k + \frac{\sigma^2}{\rho^{\text{pilot}}(L-K)})}, \quad \forall k, \quad (34)$$

$$\gamma_k^{\text{MMSE,SC}} \approx \frac{\beta_k^2}{\beta_k + \frac{\sigma^2}{\rho^{\text{pilot}}(L-K)}} \Gamma, \quad \forall k, \quad (35)$$

with Γ being the unique solution to the following equation:

$$\frac{J}{\Gamma} = \frac{1}{M} \sum_{n \in \mathcal{K}} \frac{\beta_n^2}{\beta_n + \frac{\sigma^2}{\rho^{\text{pilot}}(L-K)} + \beta_n^2 \Gamma} + \frac{1}{M} \sum_{n \in \mathcal{K}} \frac{\frac{\beta_n \sigma^2}{\rho^{\text{pilot}}(L-K)}}{\beta_n + \frac{\sigma^2}{\rho^{\text{pilot}}(L-K)}}. \quad (36)$$

V. COST OF MASSIVE DEVICE DETECTION

One of the main results from Part I of this paper [2] is that in the massive MIMO regime, user activity detection can always be made with negligible probability of error. What is then the cost of device detection? A goal of the Part II of this paper is to illustrate that the cost of device detection arises as consequence of significantly larger channel estimation error due to the use of non-orthogonal pilot sequences. This section quantifies such cost by comparing the user achievable rate as given in the previous section to the achievable rate of the widely studied massive MIMO

system with known user activity but with imperfect channel estimation. We focus on the $L > K$ regime in order to have reasonable channel estimation error. For simplicity, we ignore the issue of scheduling and assume that all active users transmit simultaneously in the second phase.

When the user activities are perfectly known at the BS, Phase I of the transmission then consists of only the K active users sending their pilot sequences to the BS for channel estimation purpose. Similar to (2), the received signal at the BS is

$$\begin{aligned} \mathbf{Y} &= \sqrt{\rho^{\text{pilot}} L} \sum_{k \in \mathcal{K}} \mathbf{a}_k \mathbf{h}_k^H + \mathbf{Z} \\ &= \sqrt{\rho^{\text{pilot}} L} \mathbf{A}_{\mathcal{K}} \mathbf{H}_{\mathcal{K}} + \mathbf{Z}, \end{aligned} \quad (37)$$

where $\mathbf{A}_{\mathcal{K}} = [\dots, \mathbf{a}_k, \dots] \in \mathbb{C}^{L \times K}$ with $\|\mathbf{a}_k\|^2 = 1$ and $\mathbf{H}_{\mathcal{K}} = [\dots, \mathbf{h}_k, \dots]^H \in \mathbb{C}^{K \times M}$ are the collections of the pilot sequences and channels for all the active users $k \in \mathcal{K}$.

Differing, however, from the massive connectivity scenario where the pilot sequences must be non-orthogonal, e.g., the entries of \mathbf{A} in (2) are generated based on the i.i.d. Gaussian distribution, in the case with prior user activity information, it is the best to assign orthogonal pilot sequences with length $L \geq K$ to the active users [10], i.e., $\mathbf{A}_{\mathcal{K}}^H \mathbf{A}_{\mathcal{K}} = \mathbf{I}$. The BS then applies matching filter, i.e., $\mathbf{A}_{\mathcal{K}}^H$, to its received signal (37), resulting in

$$\hat{\mathbf{h}}_k = \sqrt{\rho^{\text{pilot}} L} \mathbf{h}_k + (\mathbf{a}_k^H \mathbf{Z})^H, \quad \forall k \in \mathcal{K}. \quad (38)$$

Note that the equivalent noise is distributed as $(\mathbf{a}_k^H \mathbf{Z})^H \sim \mathcal{CN}(\mathbf{0}, \sigma^2 \mathbf{I})$. It can be shown that if the MMSE channel estimation is used on the channel model (38), the estimated channels and their uncorrelated channel estimation errors are distributed as $\hat{\mathbf{h}}_k \sim \mathcal{CN}\left(\mathbf{0}, \frac{\beta_k^2}{\beta_k + \sigma^2 / (\rho^{\text{pilot}} L)} \mathbf{I}\right)$ and $\Delta \mathbf{h}_k \sim \mathcal{CN}\left(\mathbf{0}, \frac{\beta_k \sigma^2 / (\rho^{\text{pilot}} L)}{\beta_k + \sigma^2 / (\rho^{\text{pilot}} L)} \mathbf{I}\right)$, $\forall k \in \mathcal{K}$, respectively [8]. Similar to Theorem 2 and by using the approximation technique used in Section IV-C, the users' rates achieved by the MRC and MMSE beamforming strategies in the regime $L > K$ can be shown to be as given in (16), where

$$\gamma_k^{\text{MRC}} \approx \frac{\beta_k^2}{\frac{1}{M} \sum_{n \in \mathcal{K}} \beta_n (\beta_k + \frac{\sigma^2}{\rho^{\text{pilot}} L})}, \quad \forall k, \quad (39)$$

$$\gamma_k^{\text{MMSE}} \approx \frac{\beta_k^2}{\beta_k + \frac{\sigma^2}{\rho^{\text{pilot}} L}} \Gamma, \quad \forall k, \quad (40)$$

with Γ being the unique solution to the following equation:

$$\begin{aligned} \frac{1}{\Gamma} &= \frac{1}{M} \sum_{n \in \mathcal{K}} \frac{\beta_n^2}{\beta_n + \frac{\sigma^2}{\rho^{\text{pilot}} L} + \beta_n^2 \Gamma} \\ &\quad + \frac{1}{M} \sum_{n \in \mathcal{K}} \frac{\frac{\beta_n \sigma^2}{\rho^{\text{pilot}} L}}{\beta_n + \frac{\sigma^2}{\rho^{\text{pilot}} L}}. \end{aligned} \quad (41)$$

Comparing to the massive connectivity scenario without prior user activity information, for which the SINRs achieved by the MRC and MMSE beamforming are given in (31) and (32), respectively, it can be observed that the

cost of user activity detection lies in the effective channel estimation error, which increases from $\frac{\sigma^2}{\rho_{\text{pilot}} L}$ to $\frac{\sigma^2}{\rho_{\text{pilot}}(L-K)}$.

As mentioned earlier, the reason for this cost is that for the massive connectivity scenario, since $L < N$, it is impossible to assign orthogonal pilot sequences to all N users. If the entries of \mathbf{A} are generated according to i.i.d. Gaussian distribution, although the user activity detection by the vector AMP algorithm is perfect due to the results in Part I of this paper [2], this choice of \mathbf{A} nevertheless results in larger channel estimation error because of multiuser interference as compared to the case where orthogonal pilot sequences can be used. This is reminiscent of the well-known inter-cell pilot contamination problem in conventional massive MIMO systems, except that the contamination now comes from the non-orthogonal pilots within the cell as the cost of supporting massive connectivity.

VI. OPTIMIZATION OF PILOT LENGTH

The characterization of the channel estimation error and user achievable rates also allows an optimization of the pilot sequence length for maximizing the system sum rate. Longer pilot sequences result in better channel estimation but shorter data transmission time, and vice versa, so there is an optimal L that balances the two effects. Again in this section, we ignore scheduling and assume that all active users transmit simultaneously in the second phase. The optimization of user scheduling is discussed in the next section.

First, consider the case with MRC beamforming at the BS. According to (16) and (31), in the practical regime of $L > K$, the sum rate maximization problem can be expressed as

$$\max_{K < L < T} \frac{T-L}{T} \sum_{k \in \mathcal{K}} \log_2 \left(1 + \frac{M\beta_k^2}{\sum_{n \in \mathcal{K}} \beta_n (\beta_k + \frac{\sigma^2}{\rho_{\text{pilot}}(L-K)})} \right) \quad (42)$$

Theorem 3: The objective function of problem (42) is a concave function over L in the range $K < L < T$, if L is relaxed as a real number.

Proof: Please refer to Appendix C. ■

According to Theorem 3, problem (42) can be globally solved as follows. First, we ignore the constraint that L is an integer and solve the relaxed convex version of problem (42). Let L^* denote the optimal solution, which is not necessarily an integer. Then, L^* either rounding up or rounding down to the next integer value would be the optimal pilot sequence length, depending on which way maximizes the user sum rate.

Next, consider the case when the MMSE beamforming is employed at the BS. According to (16) and (32), in the case of $L > K$, the sum rate maximization problem over the pilot sequence length for the MMSE beamforming case is

$$\max_{K < L < T} \frac{T-L}{T} \sum_{k \in \mathcal{K}} \log_2 \left(1 + \frac{\beta_k^2}{\beta_k + \frac{\sigma^2}{\rho_{\text{pilot}}(L-K)}} \Gamma \right) \quad (43)$$

where Γ is the solution to (33). However, since Γ is a complicated function of L , it is non-trivial to solve the problem (43). Nevertheless, the optimal pilot sequence length for the MMSE beamforming case can be obtained by a one-dimension search.

VII. OPTIMIZATION OF USER SCHEDULING

We now consider the question of in an overloaded system with more users than the number of BS antennas, what the optimal number of scheduling intervals J should be chosen as for maximizing the system sum rate. Assuming $L > K$, consider first the case of MRC beamforming at the BS. According to the user rate expressions given in (26) and (34), the sum rate maximization problem over J can be formulated as

$$\max_{J \geq 1} \frac{T-L}{TJ} \sum_{k \in \mathcal{K}} \log_2 \left(1 + \frac{JM\beta_k^2}{\sum_{n \in \mathcal{K}} \beta_n (\beta_k + \frac{\sigma^2}{\rho_{\text{pilot}}(L-K)})} \right) \quad (44)$$

Theorem 4: The objective function of problem (44) is a monotonically decreasing function over J . As a result, the optimal solution to problem (44) is $J^* = 1$.

Proof: Please refer to Appendix D. ■

Intuitively, Theorem 4 implies that under MRC, if we reduce the number of scheduled users in each interval, the sacrifice of data transmission time plays a more significant role on user sum rate than the reduction in inter-user interference. Such a phenomenon reveals the inefficiency of MRC beamforming in an overloaded system, since even user scheduling cannot improve the user sum rate.

Next, consider the case when the MMSE beamforming is employed at the BS. According to the user rate given in (28) and (35), the sum rate maximization problem over J can be formulated as

$$\max_{J \geq 1} \frac{T-L}{TJ} \sum_{k \in \mathcal{K}} \log_2 \left(1 + \frac{\beta_k^2}{\beta_k + \frac{\sigma^2}{\rho_{\text{pilot}}(L-K)}} \Gamma \right) \quad (45)$$

where Γ is the solution to (36). Since the solution to (36) is a complicated function of J , it is non-trivial to solve problem (45) analytically. However, the optimal solution to problem (45) can be easily obtained numerically via a one-dimension search.

Differing from the case of MRC beamforming at the BS, as shown later by numerical simulations, the optimal solution to problem (45) is J strictly larger than 1 in general. Thus, user scheduling can significantly improve the user sum rate when the MMSE beamforming is employed at the BS.

VIII. NUMERICAL EXAMPLES

In this section, we provide numerical examples to verify the main results of this paper. The setup is the same as in the numerical simulations in Part I of this paper. There are $N = 2000$ users in a single cell. Let d_n denote the distance between user n and the BS, $\forall n$. It is assumed that d_n 's

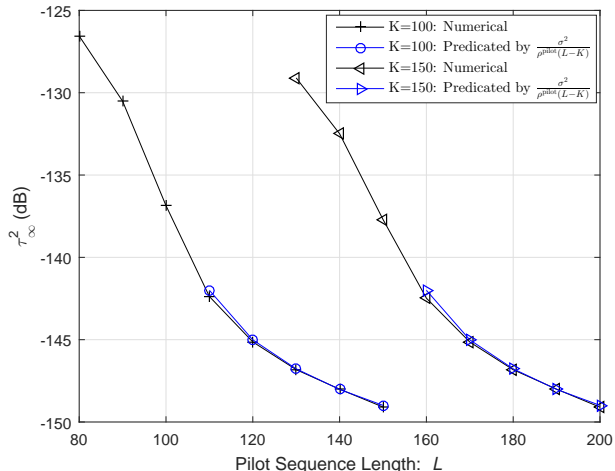


Fig. 2. Fixed point of state evolution when each of the $N = 2000$ users accesses the channel with probability $\epsilon = 0.05$ or $\epsilon = 0.075$ in each coherence time; the BS has $M = 128$ antennas, and the SNR of the farthest user is 14dB.

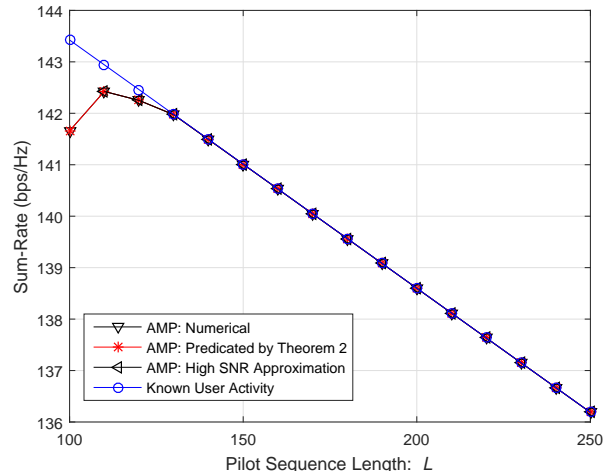
are randomly distributed in the regime $[0.05\text{km}, 1\text{km}]$. The path loss model of the wireless channel for user n is given as $\beta_n = -128.1 - 36.7 \log_{10}(d_n)$ in dB, $\forall n$. The bandwidth and the coherence time of the wireless channel are 1MHz and 1ms, respectively, thus in each coherence block $T = 1000$ symbols can be transmitted. The transmit power for each user at both the first and second transmission phases is $\rho^{\text{pilot}} = \rho^{\text{data}} = 23\text{dBm}$. The power spectral density of the AWGN at the BS is assumed to be -169dBm/Hz . Moreover, all the following numerical results are obtained by averaging over 100,000 channel realizations.

A. Fixed-Point of State Evolution for AMP

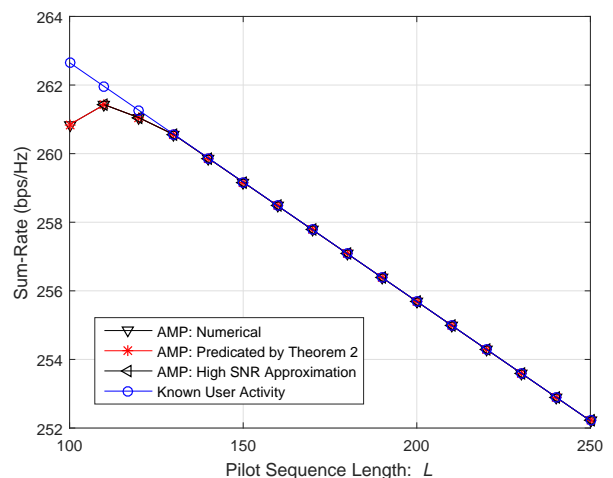
Fig. 2 shows the numerical evaluation of the fixed-point solution to the state evolution of AMP, which is used for characterizing the channel estimation error. In this numerical example, each of the N users accesses the channel with probability $\epsilon = 0.05$ or $\epsilon = 0.075$ in each coherence time (around $K = 100$ or $K = 150$ users are active), and the number of antennas at the BS is $M = 128$. Note that in this example, the SNR of the farthest user, which is 1km away from the BS, is 14dB. Fig. 2 shows the comparison between the numerical evaluation of the fixed point (8) and the high-SNR approximation given in (11) in Theorem 1 for different values of L . Note that the transmit power is set to be $\xi = L\rho^{\text{pilot}}$ so that (11) reduces to $\tau_\infty^2 = \frac{\sigma^2}{\rho^{\text{pilot}}(L-K)}$. It is observed that (11) is a very good approximation of the exact fixed-point solution in this practical SNR range when $L > K$.

B. Cost for User Activity Detection on User Rates

Next we quantify the cost of user activity detection on achievable rates. Figs. 3 and 4 show the user sum rates



(a) MRC Receive Beamforming with $M = 128$



(b) MRC Receive Beamforming with $M = 256$

Fig. 3. User sum rate comparison with MRC receive beamforming between the cases with and without prior user activity information at the BS when each of the $N = 2000$ users accesses the channel with probability $\epsilon = 0.05$ in each coherence time and the BS has $M = 128$ or 256 antennas.

versus the length of the pilot sequences L for both the cases of MRC and MMSE beamforming at the BS. In this numerical example, there are $M = 128$ or $M = 256$ antennas at the BS and each of the $N = 2000$ users accesses the channel with probability $\epsilon = 0.05$ at each coherence time (around $K = 100$ users are active). As baseline, the scenario with prior information on user activity known at the BS is also plotted, where orthogonal pilot sequences can be assigned to the active users for channel estimation in the first phase.

With the MRC beamforming at the BS, it is observed from Fig. 3 that for the case without prior information of the user activity, the theoretical result shown in Theorem 2 and the high-SNR approximation (16) and (31) both perfectly match the numerical result for various values of L .

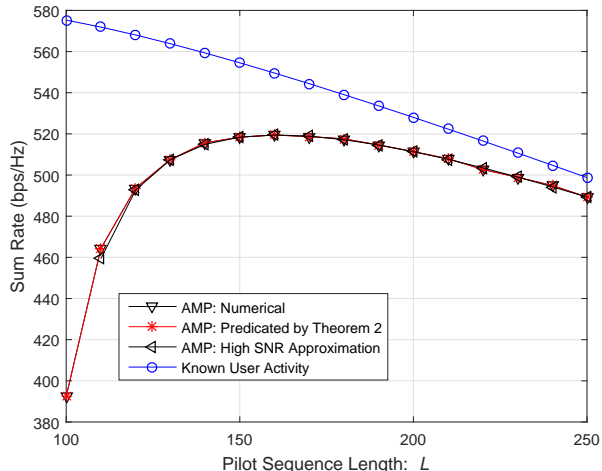
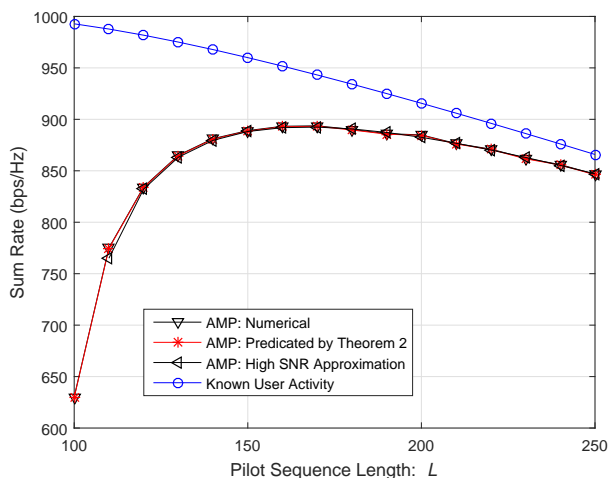
(a) MMSE Receive Beamforming with $M = 128$ (b) MMSE Receive Beamforming with $M = 256$

Fig. 4. User sum rate comparison with MMSE receive beamforming between the cases with and without prior user activity information at the BS when each of the $N = 2000$ users accesses the channel with probability $\epsilon = 0.05$ in each coherence time and the BS has $M = 128$ or $M = 256$ antennas.

Moreover, it is observed that the optimal pilot lengths are $L = K = 100$ and $L = 110$ for the cases with and without prior information of the user activity at the BS, respectively. Note that without prior information of the user activity, the MSE for channel estimation is larger, thus more time needs to be spent in the first phase to improve the channel estimation accuracy. Finally, it is observed that maximal sum rates for the cases with and without prior information of user activity at the BS are very close, indicating that the cost of user activity detection is quite small under MRC beamforming.

The user achievable rate can be dramatically improved, however, if MRC beamforming is replaced with MMSE beamforming, as shown in Fig. 4. It can be observed from Fig. 4 that with the MMSE beamforming at the BS,

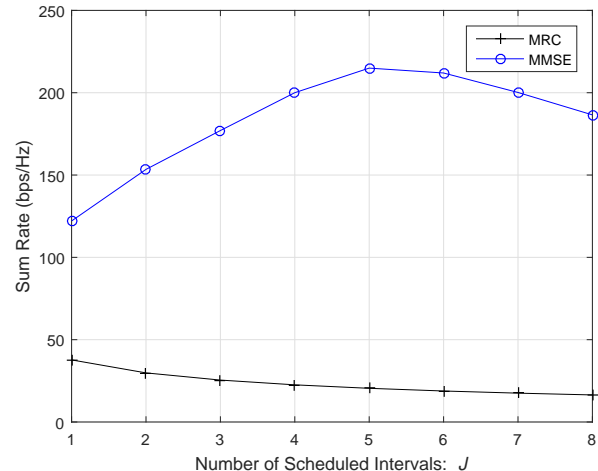


Fig. 5. User sum rate versus different numbers of scheduled intervals in the second transmission phase when each of the $N = 2000$ users accesses the channel with probability $\epsilon = 0.15$ in each coherence time and the BS has $M = 64$ antennas.

the theoretical result shown in Theorem 2 and the high-SNR approximation (16) and (32)-(33) perfectly match the numerical result for all values of L . Moreover, it is observed that the optimal pilot length is $L = 160$ when user activity is not known a priori at the BS, and the cost of user activity detection is about 10% of the overall sum rate. Note that this optimal length is much longer than that for the case with MRC beamforming, which is $L = 110$. This is because different from the MRC beamforming, the MMSE beamforming for each user is a function of the estimated channels of all the users, as shown in (19). As a result, the performance of MMSE beamforming is more sensitive to the channel estimation error, thus we should allocate more time for channel training. Given the significant sum rate improvement of MMSE beamforming over MRC beamforming, this is a small price to pay.

It is worth emphasizing that MRC is not well suited for massive connectivity applications, because as explained earlier it is unable to mitigate the significant multiuser interference stemmed from a large number of devices. The fact that MMSE beamforming is capable of achieving five or six times higher sum rate than MRC, as shown in Figs. 3 and 4, illustrates that MMSE rather than MRC beamforming should be used for massive connectivity applications, even though MRC would have been adequate in conventional massive MIMO systems.

C. The Impact of User Scheduling on User Rates

Finally, we study the impact of user scheduling in an overloaded system. In this example, we assume that there are $M = 64$ antennas at the BS and each of the $N = 2000$ users accesses the channel with probability $\epsilon = 0.15$ at each coherence time (around $K = 300$ users are active) such that $\mu = \frac{K}{M} > 1$. It is further assumed that the pilot sequence

length is $L = 400$. Fig. 5 shows the user sum rate versus the number of scheduled intervals of the data transmission phase J . For the case of MRC beamforming at the BS, it is observed that the user sum rate decreases with the number of scheduled intervals J , which verifies Theorem 4. This is in fact an indication of the inefficiency of MRC beamforming in an overloaded system. In contrast, for the MMSE beamforming, it is observed that user scheduling can significantly enhance the overall sum rate. Specifically, in this numerical example the optimal strategy is to schedule 60 users in each of $J = 5$ intervals such that for any particular interval the system is almost fully loaded. This example shows that for massive connectivity applications with massive MIMO, if the number of users is much larger than the number of antennas at the BS, combining user scheduling together with MMSE receive beamforming at the BS can be a good strategy for managing multiuser interference.

IX. CONCLUSION AND FUTURE WORK

This two-part paper illustrates that massive MIMO is ideally suited for massive connectivity applications. The main technical contribution of the overall two-part paper is a characterization of the effect of using non-orthogonal pilot sequences for massive device activity detection, channel estimation, and data transmission. The main conclusion of this Part II of the paper is that despite perfect device activity detection in the massive MIMO regime, a loss in the overall achievable transmission rate nevertheless arises as compared to the conventional massive MIMO system because of the significantly larger channel estimation error due to the non-orthogonality of pilot sequences. We also show that for massive connectivity applications, it is essential to use MMSE beamforming instead of MRC; the optimal pilot length should be longer than that in conventional massive MIMO systems in order to compensate for the additional channel estimation error; finally scheduling can enhance the overall transmission rate.

There are a number of directions along which the results of this paper can be further extended. First, we mention that power control has not been taken into account. In this paper, all the active users transmit with an identical transmit power in each of the first and second phases. It is conceivable that users far away from the BS can be assigned with higher power so that a more fair rate distribution among all the active users can be achieved. Second, this paper has not addressed the issue of optimal scheduling. Future work on how to select the active users in each scheduled interval to maximize user achievable rate will be of interest. Further, the results of this paper are restricted to single-cell scenarios. Future work can extend the existing results to account for inter-cell interference and to investigate ways to provide adequate coverage to cell-edge users.

APPENDIX

A. Proof of Theorem 1

First, we show that when $\omega\epsilon < 1$, the fixed point of the simplified state evolution

$$\tau_\infty^2 = \frac{\sigma^2}{\xi} + \omega\epsilon\mathbb{E}_\beta \left[\frac{\beta\tau_\infty^2}{\beta + \tau_\infty^2} \right], \quad (46)$$

is unique. Define

$$f(x) = x - \omega\epsilon\mathbb{E}_\beta \left[\frac{\beta x}{\beta + x} \right] - \frac{\sigma^2}{\xi}, \quad x \geq 0. \quad (47)$$

It can be easily shown that $f(x)$ is a continuous function of x . Moreover, the derivative of $f(x)$ is

$$f'(x) = 1 - \omega\epsilon\mathbb{E}_\beta \left[\frac{\beta^2}{(\beta + x)^2} \right], \quad x \geq 0. \quad (48)$$

When $\omega\epsilon < 1$, we have $f'(x) \geq 0$, thus $f(x)$ is a monotonically increasing function for $x \in [0, \infty)$. Consequently, the fixed point of (46) is unique.

Second, we show that the fixed-point solution of (46) is bounded by (10) if $\omega\epsilon < 1$. It can be easily seen from (46) that $\tau_\infty^2 \geq \sigma^2/\xi$. Moreover, we have

$$\tau_\infty^2 = \frac{\sigma^2}{\xi} + \omega\epsilon\mathbb{E}_\beta \left[\frac{\beta\tau_\infty^2}{\beta + \tau_\infty^2} \right] \leq \frac{\sigma^2}{\xi} + \omega\epsilon\tau_\infty^2, \quad (49)$$

where the inequality is because $\beta\tau_\infty^2/(\beta + \tau_\infty^2) \leq \tau_\infty^2, \forall \beta \geq 0$. As a result, if $\omega\epsilon < 1$, it follows that $\tau_\infty^2 \leq \sigma^2/((1 - \omega\epsilon)\xi)$.

Next, we verify that when $\frac{\xi\beta_{\min}}{\sigma^2} \rightarrow \infty$,

$$\tau_\infty^2 = \frac{\sigma^2}{\xi(1 - \omega\epsilon)} \quad (50)$$

is a fixed-point solution of (46). Substituting the above τ_∞^2 into the right-hand side of the simplified state evolution, we have

$$\begin{aligned} \frac{\sigma^2}{\xi} + \omega\epsilon\mathbb{E}_\beta \left[\frac{\beta\tau_\infty^2}{\beta + \tau_\infty^2} \right] &= \frac{\sigma^2}{\xi} + \frac{\sigma^2\omega\epsilon}{\xi(1 - \omega\epsilon)}\mathbb{E}_\beta \left[\frac{1}{1 + \frac{\sigma^2}{\beta\xi(1 - \omega\epsilon)}} \right] \\ &\rightarrow \frac{\sigma^2}{\xi} + \frac{\sigma^2\omega\epsilon}{\xi(1 - \omega\epsilon)} \\ &= \frac{\sigma^2}{\xi(1 - \omega\epsilon)} = \tau_\infty^2, \end{aligned} \quad (51)$$

where the second last line is due to the high SNR assumption and that $\omega\epsilon < 1$. This verifies that (50) is the unique solution to (46) in the high SNR limit.

B. Proof of Theorem 2

With the MRC beamforming given in (18), it can be shown that the SINR of user k given in (17) reduces to

$$\gamma_k^{\text{MRC}} = \frac{\rho^{\text{data}} \|\hat{\mathbf{h}}_k\|^4}{\rho^{\text{data}} \sum_{n \in \mathcal{K}, n \neq k} |\hat{\mathbf{h}}_k^H \hat{\mathbf{h}}_n|^2 + \rho^{\text{data}} \|\hat{\mathbf{h}}_k\|^2 \sum_{n \in \mathcal{K}} \frac{\beta_n \tau_\infty^2}{\beta_n + \tau_\infty^2} + \sigma^2 \|\hat{\mathbf{h}}_k\|^2}. \quad (52)$$

If the estimated channels are distributed as $\hat{\mathbf{h}}_n \sim \mathcal{CN}(\mathbf{0}, \frac{\beta_k^2}{\beta_n + \tau_\infty^2} \mathbf{I})$, $\forall n \in \mathcal{K}$, as $M \rightarrow \infty$, it thus follows that

$$\frac{\|\hat{\mathbf{h}}_k\|^2}{M} \rightarrow \left(\frac{\beta_k^2}{\beta_k + \tau_\infty^2} \right), \quad (53)$$

and

$$\frac{\|\hat{\mathbf{h}}_k\|^2 \sum_{n \in \mathcal{K}} \frac{\beta_n \tau_\infty^2}{\beta_n + \tau_\infty^2}}{KM} \rightarrow \mathbb{E} \left[\frac{\beta \tau_\infty^2}{\beta + \tau_\infty^2} \right] \left(\frac{\beta_k^2}{\beta_k + \tau_\infty^2} \right). \quad (54)$$

Moreover, according to Appendix B in [13], we have

$$\frac{\sum_{n \in \mathcal{K}, n \neq k} |\hat{\mathbf{h}}_k^H \hat{\mathbf{h}}_n|^2}{KM} \rightarrow \mathbb{E} \left[\frac{\beta^2}{\beta + \tau_\infty^2} \right] \frac{\beta_k^2}{\beta_k + \tau_\infty^2}. \quad (55)$$

As a result, as $M \rightarrow \infty$, each active user's achievable SINR converges to

$$\begin{aligned} \gamma_k^{\text{MRC}} &\rightarrow \frac{\rho^{\text{data}} M^2 \left(\frac{\beta_k^2}{\beta_k + \tau_\infty^2} \right)^2}{\rho^{\text{data}} K M \mathbb{E} \left[\frac{\beta^2}{\beta + \tau_\infty^2} + \frac{\beta \tau_\infty^2}{\beta + \tau_\infty^2} \right] \left(\frac{\beta_k^2}{\beta_k + \tau_\infty^2} \right) + \sigma^2 M \left(\frac{\beta_k^2}{\beta_k + \tau_\infty^2} \right)} \\ &\rightarrow \frac{\beta_k^2}{\mu \mathbb{E}[\beta] (\beta_k + \tau_\infty^2)}, \quad \forall k, \end{aligned} \quad (56)$$

thus establishing (20).

With the MMSE beamforming given in (19), it can be shown that the SINR of user k given in (17) reduces to

$$\begin{aligned} \gamma_k^{\text{MMSE}} &= \rho^{\text{data}} \hat{\mathbf{h}}_k^H \left(\sum_{n \in \mathcal{K}, n \neq k} \rho^{\text{data}} \hat{\mathbf{h}}_n \hat{\mathbf{h}}_n^H \right. \\ &\quad \left. + \sum_{n \in \mathcal{K}} \frac{\rho^{\text{data}} \beta_n \tau_\infty^2}{\beta_n + \tau_\infty^2} \mathbf{I} + \sigma^2 \mathbf{I} \right)^{-1} \hat{\mathbf{h}}_k. \end{aligned} \quad (57)$$

If the estimated channels are distributed as $\hat{\mathbf{h}}_k \sim \mathcal{CN}(\mathbf{0}, \frac{\beta_k^2}{\beta_k + \tau_\infty^2} \mathbf{I})$, $\forall k \in \mathcal{K}$, as $M \rightarrow \infty$, it thus follows that

$$\begin{aligned} \gamma_k^{\text{MMSE}} &\rightarrow \frac{\rho^{\text{data}} \beta_k^2}{M(\beta_k + \tau_\infty^2)} \text{tr} \left(\left(\sum_{n \in \mathcal{K}, n \neq k} \frac{\rho^{\text{data}} \hat{\mathbf{h}}_n \hat{\mathbf{h}}_n^H}{M} \right. \right. \\ &\quad \left. \left. + \sum_{n \in \mathcal{K}} \frac{\rho^{\text{data}} \beta_n \tau_\infty^2}{M(\beta_n + \tau_\infty^2)} \mathbf{I} + \frac{\sigma^2}{M} \mathbf{I} \right)^{-1} \right) \end{aligned} \quad (58)$$

$$\begin{aligned} &\rightarrow \frac{\rho^{\text{data}} \beta_k^2}{M(\beta_k + \tau_\infty^2)} \text{tr} \left(\left(\sum_{n \in \mathcal{K}} \frac{\rho^{\text{data}} \hat{\mathbf{h}}_n \hat{\mathbf{h}}_n^H}{M} \right. \right. \\ &\quad \left. \left. + \sum_{n \in \mathcal{K}} \frac{\rho^{\text{data}} \beta_n \tau_\infty^2}{M(\beta_n + \tau_\infty^2)} \mathbf{I} + \frac{\sigma^2}{M} \mathbf{I} \right)^{-1} \right) \end{aligned} \quad (59)$$

$$\begin{aligned} &\rightarrow \frac{\rho^{\text{data}} \beta_k^2}{M(\beta_k + \tau_\infty^2)} \text{tr} \left(\left(\sum_{n \in \mathcal{K}} \frac{\rho^{\text{data}} \beta_n^2}{M(1 + e_n)(\beta_n + \tau_\infty^2)} \mathbf{I} \right. \right. \\ &\quad \left. \left. + \sum_{n \in \mathcal{K}} \frac{\rho^{\text{data}} \beta_n \tau_\infty^2}{M(\beta_n + \tau_\infty^2)} \mathbf{I} + \frac{\sigma^2}{M} \mathbf{I} \right)^{-1} \right) \end{aligned} \quad (60)$$

$$\rightarrow \frac{\beta_k^2}{\beta_k + \tau_\infty^2} \cdot \frac{1}{\mu \mathbb{E} \left[\frac{\beta^2}{(1+e)(\beta + \tau_\infty^2)} \right] + \mu \mathbb{E} \left[\frac{\beta \tau_\infty^2}{\beta + \tau_\infty^2} \right] + \frac{\sigma^2}{M \rho^{\text{data}}}} \quad (61)$$

$$\rightarrow \frac{\beta_k^2}{\beta_k + \tau_\infty^2} \cdot \frac{1}{\mu \mathbb{E} \left[\frac{\beta^2}{(1+e)(\beta + \tau_\infty^2)} \right] + \mu \mathbb{E} \left[\frac{\beta \tau_\infty^2}{\beta + \tau_\infty^2} \right]}, \quad (62)$$

where

$$\begin{aligned} e_k &= \frac{1}{M} \text{tr} \left(\mathbb{E} \left(\rho^{\text{data}} \hat{\mathbf{h}}_k \hat{\mathbf{h}}_k^H \right) \left(\sum_{n \in \mathcal{K}} \frac{\mathbb{E} \left(\rho^{\text{data}} \hat{\mathbf{h}}_n \hat{\mathbf{h}}_n^H \right)}{M(1 + e_n)} \right. \right. \\ &\quad \left. \left. + \sum_{n \in \mathcal{K}} \frac{\rho^{\text{data}} \beta_n \tau_\infty^2}{M(\beta_n + \tau_\infty^2)} \mathbf{I} + \frac{\sigma^2}{M} \mathbf{I} \right)^{-1} \right) \\ &\rightarrow \frac{\rho^{\text{data}} \beta_k^2}{M(\beta_k + \tau_\infty^2)} \text{tr} \left(\left(\sum_{n \in \mathcal{K}} \frac{\rho^{\text{data}} \beta_n^2}{M(1 + e_n)(\beta_n + \tau_\infty^2)} \mathbf{I} \right. \right. \\ &\quad \left. \left. + \sum_{n \in \mathcal{K}} \frac{\rho^{\text{data}} \beta_n \tau_\infty^2}{M(\beta_n + \tau_\infty^2)} \mathbf{I} + \frac{\sigma^2}{M} \mathbf{I} \right)^{-1} \right) \\ &\rightarrow \gamma_k^{\text{MMSE}}. \end{aligned} \quad (63)$$

In the above, (58) is due to [14, Lemma 4], (59) is due to [14, Lemma 6], (60) is due to [14, Theorem 1], and (63) is due to (60).

As a result, the user SINRs are the fixed-point solution to the following equations:

$$\begin{aligned} \gamma_k^{\text{MMSE}} &= \frac{\beta_k^2}{\beta_k + \tau_\infty^2} \cdot \frac{1}{\mu \mathbb{E} \left[\frac{\beta^2}{(1 + \gamma^{\text{MMSE}})(\beta + \tau_\infty^2)} + \frac{\beta \tau_\infty^2}{\beta + \tau_\infty^2} \right]}, \quad \forall k \in \mathcal{K}. \end{aligned} \quad (64)$$

Define

$$\Gamma = \frac{1}{\mu \mathbb{E} \left[\frac{\beta^2}{(1 + \Gamma)(\beta + \tau_\infty^2)} + \frac{\beta \tau_\infty^2}{\beta + \tau_\infty^2} \right]}. \quad (65)$$

Then, (64) reduces to

$$\gamma_k^{\text{MMSE}} = \frac{\beta_k^2}{\beta_k + \tau_\infty^2} \cdot \Gamma, \quad \forall k \in \mathcal{K}. \quad (66)$$

By taking (66) into both the left-hand side and right-hand side of the equation given in (64), it can be shown that Γ is the fixed-point solution to the following equation:

$$\Gamma = \frac{1}{\mu \mathbb{E} \left[\frac{\beta^2}{(1 + \frac{\beta^2}{\beta + \tau_\infty^2} \times \Gamma)(\beta + \tau_\infty^2)} + \frac{\beta \tau_\infty^2}{\beta + \tau_\infty^2} \right]} \quad (67)$$

$$= \frac{1}{\mu \mathbb{E} \left[\frac{\beta^2}{\beta + \tau_\infty^2 + \beta^2 \Gamma} \right] + \mu \mathbb{E} \left[\frac{\beta \tau_\infty^2}{\beta + \tau_\infty^2} \right]}. \quad (68)$$

At last, we prove the uniqueness of the fixed-point solution to (22). First, it can be observed that $\Gamma = 0$ is not the fixed-point solution. Divide both the left-hand side and right-hand side of (22) by Γ and consider the following function:

$$f(\Gamma) = \frac{1}{\mu\mathbb{E}\left[\frac{\beta^2\Gamma}{\beta+\tau_\infty^2+\beta^2\Gamma}\right] + \mu\mathbb{E}\left[\frac{\beta\tau_\infty^2\Gamma}{\beta+\tau_\infty^2}\right]} - 1. \quad (69)$$

It can be shown that $f(\Gamma)$ is a decreasing function over Γ when $\Gamma \geq 0$. Moreover, we have $f(\Gamma \rightarrow \infty) \rightarrow -1 < 0$ and $f(\Gamma = 0) \rightarrow \infty > 0$. As a result, there must be a unique finite solution to $f(\Gamma) = 0$, which is the unique finite fixed-point solution to (22).

Theorem 2 is thus proved.

C. Proof of Theorem 3

Suppose L is relaxed as a real number. For convenience, define

$$f_k(L) = \log_2 \left(1 + \frac{\beta_k^2}{\frac{1}{M} \sum_{n \in \mathcal{K}} \beta_n (\beta_k + \frac{\sigma^2}{\rho^{\text{pilot}}(L-K)})} \right), \quad (70)$$

$$f(L) = \sum_{k \in \mathcal{K}} f_k(L), \quad (71)$$

$$g(L) = \frac{T-L}{T} f(L). \quad (72)$$

Note that $g(L)$ is the objective function of problem (42).

First, we study the function $f_k(L)$. Define

$$a_k = \beta_k^2 + \frac{1}{M} \sum_{n \in \mathcal{K}} \beta_n \beta_k, \quad \forall k \in \mathcal{K}. \quad (73)$$

It can be shown that the first-order derivative of $f_k(L)$ is

$$\begin{aligned} f'_k(L) &= \frac{\frac{\beta_k^2 \sigma^2}{\rho^{\text{pilot}} \log 2}}{\left(a_k(L-K) + \frac{\frac{1}{M} \sum_{n \in \mathcal{K}} \beta_n \sigma^2}{\rho^{\text{pilot}}} \right) \left(\beta_k(L-K) + \frac{\sigma^2}{\rho^{\text{pilot}}} \right)} \\ &> 0, \quad \text{if } L > K. \end{aligned} \quad (74)$$

Moreover, it can be observed that $f'_k(L)$ is a monotonically decreasing function of L if $L > K$. As a result, it follows that $f''_k(L) < 0, \forall k$. It then follows that $f'(L) > 0$ and $f''(L) < 0$ when $L > K$.

Next, we study the function $g(L)$. It can be shown that the first and second-order derivatives of $g(L)$ are

$$g'(L) = \frac{-f(L) + (T-L)f'(L)}{T}, \quad (75)$$

$$g''(L) = \frac{-2f'(L) + (T-L)f''(L)}{T}. \quad (76)$$

Since $f'(L) > 0$ and $f''(L) < 0$, it then follows that $g''(L) < 0$ when $L/K > 1$. As a result, if L is relaxed as a real number, the objective function of problem (42) is a concave function of L when $L/K > 1$. Theorem 3 is thus proved.

D. Proof of Theorem 4

For convenience, define $x = 1/J$. Then, according to (26) and (27), the rate of user k is given as

$$f_k(x) = \frac{(T-L)x}{T} \log_2 \left(1 + \frac{M\beta_k^2}{\sum_{n \in \mathcal{K}} \beta_n (\beta_k + \frac{\sigma^2}{\rho^{\text{pilot}}(L-K)})} x \right). \quad (77)$$

Let us first ignore the constraint that J is an integer, thus x is a continuous variable. In this case, it can be shown that the first-order derivative of $f_k(x)$ is

$$\begin{aligned} f'_k(x) &= \frac{T-L}{T} \log_2 \left(1 + \frac{\beta_k^2}{\frac{1}{M} \sum_{n \in \mathcal{K}} \beta_n (\beta_k + \frac{\sigma^2}{\rho^{\text{pilot}}(L-K)})} x \right) \\ &\quad - \frac{T-L}{T \ln 2} \frac{\beta_k^2}{\frac{1}{M} \sum_{n \in \mathcal{K}} \beta_n (\beta_k + \frac{\sigma^2}{\rho^{\text{pilot}}(L-K)})} x + \beta_k^2. \end{aligned} \quad (78)$$

Moreover, the second-order derivative of $f_k(x)$ is

$$\begin{aligned} f''_k(x) &= -\frac{T-L}{T \ln 2} \frac{\beta_k^4}{\left[\frac{1}{M} \sum_{n \in \mathcal{K}} \beta_n (\beta_k + \frac{\sigma^2}{\rho^{\text{pilot}}(L-K)}) x + \beta_k^2 \right]^2} \\ &< 0. \end{aligned} \quad (79)$$

As a result, $f'_k(x)$ is a decreasing function of x . It can be shown that $f'_k(x \rightarrow \infty) \rightarrow 0$. It then follows that $f'_k(x) > f'_k(x \rightarrow \infty) = 0$, i.e., $f_k(x)$ is an increasing function of x . Note that $x = 1/J$, it thus follows that each user's rate is a decreasing function of J . In other words, $J = 1$ maximizes each user's rate. Consequently, the objective function of problem (44) is a decreasing function over J and the optimal solution to problem (44) is $J^* = 1$. Theorem 4 is thus proved.

REFERENCES

- [1] L. Liu and W. Yu, "Massive device connectivity with massive MIMO," in *Proc. IEEE Inter. Symp. Inf. Theory (ISIT)*, Jun. 2017.
- [2] L. Liu and W. Yu, "Massive connectivity with massive MIMO-Part I: Device activity detection and channel estimation," *IEEE Trans. Signal Process.*, 2018, to be published.
- [3] D. L. Donoho, A. Maleki, and A. Montanari, "Message-passing algorithms for compressed sensing," *Proc. Nat. Acad. Sci.*, vol. 106, no. 45, pp. 18914-18918, Nov. 2009.
- [4] J. Kim, W. Chang, B. Jung, D. Baron, and J. C. Ye, "Belief propagation for joint sparse recovery," Feb. 2011, [Online] Available: <http://arxiv.org/abs/1102.3289>.
- [5] M. Bayati and A. Montanari, "The dynamics of message passing on dense graphs, with applications to compressed sensing," *IEEE Trans. Inf. Theory*, vol. 57, no. 2, pp. 764-785, Feb. 2011.
- [6] S. Rangan, "Generalized approximate message passing for estimation with random linear mixing," in *Proc. IEEE Int. Symp. Inf. Theory (ISIT)*, Jul. 2011, pp. 2168-2172.
- [7] T. L. Marzetta, "Noncooperative cellular wireless with unlimited numbers of base station antennas," *IEEE Trans. Wireless Commun.*, vol. 9, no. 11, pp. 3590-3660, Nov. 2010.
- [8] H. Q. Ngo, E. G. Larsson, and T. L. Marzetta, "Energy and spectral efficiency of very large multiuser MIMO systems," *IEEE Trans. Commun.*, vol. 61, no. 4, pp. 1436-1449, Apr. 2013.
- [9] E. G. Larsson, F. Tufvesson, O. Edfors, and T. L. Marzetta, "Massive MIMO for next generation wireless systems," *IEEE Commun. Mag.*, vol. 52, no. 2, pp. 186-195, Feb. 2014.

- [10] B. Hassibi and B. M. Hochwald, "How much training is needed in multiple-antenna wireless links," *IEEE Trans. Inf. Theory*, vol. 49, no. 4, pp. 951-963, Apr. 2003.
- [11] J. Hoydis, S. Brink, and M. Debbah, "Massive MIMO in the UL/DL of cellular networks: How many antennas do we need," *IEEE J. Sel. Areas Commun.*, vol. 31, no. 2, pp. 160-171, Feb. 2013.
- [12] J. Choi, D. J. Love, and P. Bidigare, "Downlink training techniques for FDD massive MIMO systems: Open-loop and closed-loop training with memory," *IEEE J. Sel. Topics Signal Process.*, vol. 8, no. 5, pp. 802-814, Oct. 2014.
- [13] D. Tse and S. Hanly, "Linear multiuser receivers: Effective interference, effective bandwidth and capacity," *IEEE Trans. Inf. Theory*, vol. 45, no. 2, pp. 641-675, Mar. 2011.
- [14] S. Wagner, R. Couillet, M. Debbah, and D. T. M. Slock, "Large system analysis of linear precoding in correlated MISO broadcast channels under limited feedback," *IEEE Trans. Inf. Theory*, vol. 58, no. 7, pp. 4509-4537, Jul. 2012.